Catalysis Science & Technology

ROYAL SOCIETY OF CHEMISTRY

PAPER

View Article Online
View Journal | View Issue

Open Access Article. Published on 11 2568. Downloaded on 17/5/2569 10:50:58.
This article is licensed under a Creative Commons Attribution-NonCommercial 3.0 Unported Licence.

Check for updates

Cite this: *Catal. Sci. Technol.*, 2025, **15**, 5747

Hydrogen production through photocatalytic acceptorless alcohol dehydrogenation with a homogeneous nickel complex

Eman Mohamad and Darrin Richeson *

Received 29th May 2025,
Accepted 3rd August 2025

DOI: 10.1039/d5cy00647c

rsc.li/catalysis

The need for sustainable hydrogen production has driven the search for efficient, earth-abundant catalysts. We report a breakthrough in photocatalytic acceptorless alcohol dehydrogenation (AAD) using a well-defined, air-stable nickel(II) complex, $[Ni(2,6\text{-}\{Ph_2PNH\}_2(NC_5H_3))Br]^+$ ($\mathbf{1}^+$) which represents the first fully characterized nickel complex to catalyze photocatalytic AAD. This catalyst operates at room temperature under visible light irradiation to selectively produce hydrogen from various aliphatic alcohols. Catalyst performance is significantly enhanced by introducing dimethylethanolamine (DMEA) as an efficient electron donor, an electron donor previously unexplored in photoredox reactions. Mechanistic studies, supported by computational analysis, reveal the crucial role of the flexible pincer ligand in facilitating the catalytic cycle. The proposed transformation of the "PN^3P" ligand to a bidentate PN configuration, supported by DFT optimization, creates an open coordination environment at the nickel centre, key for β-hydrogen elimination. This work addresses challenges in hydrogen production and bridges the gap between traditional catalysis and photoredox chemistry and represents a significant step towards more economical and environmentally friendly hydrogen generation.

Introduction

The global energy landscape must shift towards sustainable and renewable technologies to meet future demands. Hydrogen, as a promising renewable energy source, has gained significant attention due to its potential to reduce dependence on fossil fuels and address environmental challenges.[1–3] However, current hydrogen production methods are predominantly fossil fuel-based, resulting in substantial CO_2 emissions.[4,5] Additional obstacles to implementation of hydrogen as a clean energy source are connected to safety issues with the transport and storage of hydrogen. To overcome these limitations, direct dehydrogenation of alcohols has emerged as a promising avenue for clean hydrogen production. This approach offers the potential for reversible hydrogen storage using stable organic compound such as methanol and other alcohols as hydrogen carriers. Particularly attractive are alcohols derived from biomass, such as ethanol and polyols, which can serve as renewable, stable, and high-density hydrogen storage compounds.[6]

Recent advances in the application of homogeneous molecular complexes in this field include the ruthenium-catalyzed aqueous dehydrogenation of methanol and the direct catalytic acceptorless dehydrogenation of alcohols (AAD), which generates hydrogen alongside corresponding aldehydes or ketones.[7,8] The potential of homogeneous molecular catalysts for AAD has been reviewed and reveals the dominance of Ru and Ir complexes in this field.[6,9–13]

There has been recent increased focus on the use of 3d metal complexes in such processes.[14–16] Since the dehydrogenation of alcohols is endothermic, the reported reaction conditions generally involve elevated temperatures (>90 °C) which favor the entropic term in the free energy.[17–22]

Sustainability for this transformation demands the switch to 3d metal complexes as AAD catalysts.[15,23] Examples of such complexes shown as **I** and **II** in Scheme 1. The "PN^3P" pincer ligand-supported Mn

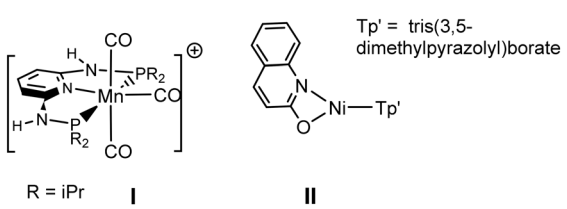

Scheme 1 Characterized 3d metal complexes for thermally activated AAD.

Department of Chemistry and Biomolecular Sciences, Centre for Catalysis Research and Innovation, University of Ottawa, 10 Marie Curie, Ottawa, ON K1N 6N5, Canada. E-mail: darrin@uottawa.ca

Open Access Article. Published on 11 2568. Downloaded on 17/5/2569 10:50:58.
This article is licensed under a Creative Commons Attribution-NonCommercial 3.0 Unported Licence.

complex **I** was primarily employed in hydrogenation of carbonyl compounds and was also noted to promote dehydrogenation at 110 °C in toluene with ^{t}BuOK base.[24] A nickel(II) complex, **II**, bearing a tris(3,5-dimethylpyrazolyl) borate ligand and a 2-hydroxyquinoline ancillary ligand, catalyzed the acceptorless dehydrogenation of alcohols in refluxing toluene, although the H_2 was not measured.[25] Efforts in electrochemically promoting the oxidation of alcohols is an alternative option employing more uses of 3d metal complexes.[26–28]

The application of visible light to activate AAD is appealing regarding cleanliness and sustainability. Light-driven alcohol splitting into H_2, and a carbonyl product remains still an important challenge. The literature has focused primarily on heterogeneous catalyst and molecular complexes remain rare.[13,29–33] Among the noble metals, a Ru(II) NHC complex was reported to catalyze the photodehydration of benzylic alcohols under basic conditions,[33] and Rh(III) polypyridyl complexes[30] and binuclear Pt(II) diphosphite complexes[31] are reported visible-light-driven alcohol dehydrogenation catalysts. Molecular photocatalysts with 3d metal centers are limited to the report of a mixture of $Ni(OAc)_2$, mercaptopropionic acid and Eosin Y for photocatalytic dehydrogenation of benzylic alcohols[34] and the AAD of aliphatic secondary alcohols with a ternary hybrid catalyst system comprising a photoredox catalyst, a thiophosphate organocatalyst, and a nickel(II) salt.[29]

Neutral chelating *N*,*N*′-bis(diorganophosphino)-2,6-diaminopyridine (2,6-{R_2PNR'}$_2$(NC_5H_3) = PN^3P) pincer ligands offer kinetic stability, coordination flexibility, tunablity of sterics and electronic properties and are known to support catalysts for variety of reactions.[15,35–38] Our previous work using complexes of PN^3P for electrocatalytic hydrogen production led to our postulating that the non-innocent behavior of the pincer ligand could be exploited for a pioneering photoredox promoted AAD reactions. For example, PN^3P-supported Co(II) catalysts demonstrated efficient electrocatalytic production of hydrogen from water with a 96% Faradaic efficiency.[39,40] Furthermore, PN^3P-supported Ni(II) complexes are active catalyst for water reduction, boasting excellent Faradaic efficiency.[41] The proposed mechanisms for these reactions rely on the non-innocent role of these ligands.

We now report the discovery that air-stable, pseudo-square-planar Ni(II) complexes, [Ni(2,6-{Ph_2PNR}$_2$(NC_5H_3))Br]$^+$ (R = H, $\mathbf{1}^+$; R = Me, $\mathbf{2}^+$), serve as an exceptional visible-light photoredox catalysts for the selective production of hydrogen. These novel complexes not only demonstrate remarkable AAD reactivity but also represents a breakthrough as the first fully characterized Ni complexes to catalyze acceptorless alcohol dehydrogenation *via* photocatalysis. The unique structure and reactivity of these complexes present new opportunities in sustainable hydrogen generation, bridging traditional catalysis and photoredox chemistry.

Results and discussion

Ready access to the PN^3P complex of Ni(II), $\mathbf{1}^+$, was provided by direct reaction of the ligand and a suspension of anhydrous $NiBr_2$. The orange complex yielded an X-ray crystal structure consisted of the distorted square-planar Ni(II) cationic complex [Ni(2,6-{Ph_2PNH}$_2$(NC_5H_3)Br]$^+$ ($\mathbf{1}^+$) with a charge balancing bromide anion as represented in Scheme 2.[41]

The exploration of the photocatalytic AAD ability of $\mathbf{1}^+$ began with methanol as a substrate and employed a typical multicomponent system consisting of a photosensitizer (PS), an electron donor (ED) and $\mathbf{1}^+$ in acetonitrile as solvent. Specifically, the PS, $Ru(bpy)_3^{2+}PF_6^-$, and **1Br** were combined with triethanol amine (TEOA), as the ED, in a glass vial with 4 ml of CH_3CN and 1 ml of methanol which was purged with N_2. The reaction mixture was irradiated with visible blue light LED for 24 h at room temperature. Gas chromatographic analysis revealed the exclusive formation of H_2, with no other gaseous products detected, demonstrating that $\mathbf{1}^+$ functioned as an excellent visible-light photoredox catalyst for selective hydrogen production (Table 1). The requirements for each of the reaction components were demonstrated by a series of control experiments. Specifically, no hydrogen was generated by catalyst systems that were not irradiated with blue light. The requirement for the presence of both the Ni complex $\mathbf{1}^+$ and the $Ru(bpy)_3^{2+}$ photosensitizer was demonstrated by background experiments carried out in the absence of one of these species and resulted in only traces of H_2 (Table 1, entries 5–7). Finally, no hydrogen was generated in the absence of an ED.

The important role of reaction solvent was demonstrated by comparing this reaction in two solvents commonly employed in photocatalytic investigations: CH_3CN and dimethylacetamide (DMA). For this catalyst system, using DMA as the reaction solvent led to increased hydrogen production by a factor greater than 2.5 as shown in Table 1 (entries 1, 2).

Tertiary aliphatic amines represent the most employed electron donors in photochemical reductions with triethanol amine (TEOA), despite the difficulty in handling this viscous liquid, being exemplar.[42] Our initial attempts with TEOA gave encouraging results (Tables 1 and S1). During these experiments we considered the role of adventitious water arising from the TEOA. The role of trace water in related heterogeneous photocatalytic reactions is of current active interest.[43] A comparison as-received TEOA with TEOA that

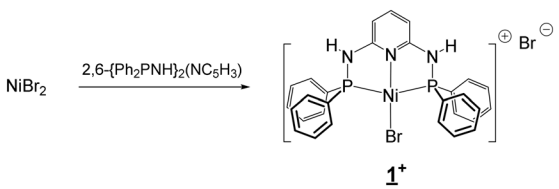

$\mathbf{1}^+$

Scheme 2 Preparation and structural representation of complex $\mathbf{1}^+$.

 This journal is © The Royal Society of Chemistry 2025

Open Access Article. Published on 11 2568. Downloaded on 17/5/2569 10:50:58.
This article is licensed under a Creative Commons Attribution-NonCommercial 3.0 Unported Licence.

Table 1 Summary of the photocatalytic acceptorless dehydrogenation of methanol using [Ni(2,6-$(Ph_2PNH)_2(NC_5H_3)$)Br]Br, **1Br**. Irradiation of 4 mL solutions of **1Br** with 2 mM $Ru(bpy)_3(PF_6)_2$ with electron donor (ED) and 1 mL added MeOH under N_2 for 24 h

Entry	[**1Br**] (mM)	Solvent	ED	MeOH	H_2 (μmol)	TON	Φ^e (%)
1	2	CH_3CN	TEOA[c]	1	101	10	0.7
2	2	DMA[b]	TEOA	1	261	26	1.6
3	2	CH_3CN	DMEA[d]	1	192	19	1.2
4	2	DMA	DMEA	1	459	46	2.9
5	0	DMA	TEOA	1	16	—	—
6	0	DMA	DMEA	1	17	—	—
7[a]	2	DMA	DMEA	1	0	—	—
8	3	DMA	DMEA	1	518	52	3.5

[a] No added $Ru(bpy)_3(PF_6)_2$. [b] DMA = dimethylacetamide. [c] Triethanolamine. [d] Dimethylethanolamine. [e] 1.84×10^{-7} mol photons per s.

had been dried using 4A molecular sieves for the photocatalytic hydrogen generation catalyzed by **1Br** revealed the deleterious effect of water on this reaction. Furthermore, the ability of simpler triethylamine (TEA) to serve as an electron donor in this reaction was examined (Table S1) and found to be successful but inferior to TEOA.

In our quest for a more accessible and cost-effective electron donor (ED), we identified dimethylethanolamine (DMEA) as a promising candidate for catalytic photoredox AAD. DMEA, an industrially produced compound, finds widespread use in applications ranging from polyurethane production catalysis to CO_2 capture.[44,45] Its lower viscosity compared to TEOA offers practical advantages in handling and application. Surprisingly, despite its potential, DMEA has not been previously reported as an electron donor in photoredox reactions. This oversight presented an opportunity to explore its efficacy in our system. As seen in Table 1, DMEA offered superior performance to TEOA in the $\mathbf{1}^+$ catalyzed photoredox activated AAD in both CH_3CN and DMA (entries 3 and 4) with significantly greater H_2 production in DMA.

It is also noteworthy that an increase in [$\mathbf{1}^+$] (entry 8) led to increase in the level of hydrogen production. This is further evidence of the catalytic role of $\mathbf{1}^+$.

Other aliphatic alcohols were also determined to be effective substrates for this photocatalyzed transformation. Successful AAD was carried out with ethanol, isopropanol, neopentyl alcohol and methanol-d[3] using the optimized conditions obtained with methanol (Table 2). Specifically, with $Ru(bpy)_3^{2+}PF_6^-$ and DMEA in DMA and blue light irradiation, $\mathbf{1}^+$ generated H_2 with a trend in production of MeOH═CD_3OH > EtOH ≥ NpOH > ^{i}PrOH. This data suggests that increased substitution on the α-C center led to slower reaction. This may be a steric effect or due to modulation of the OH bond strength.[46] Furthermore, application of this photocatalyst system to phenol, an alcohol lacking an α-hydrogen, resulted in no hydrogen generation and supported the need for these active H centers.

Employing isopropanol (iPrOH) as a substrate in this **1Br** photocatalyzed AAD provided a straightforward method for analyzing both hydrogen production and the ketone byproduct and confirming mass balance. Our results showed that 340 μmol of H_2 was generated, while 330 μmol of acetone (97% of theoretical) was produced (Fig. S3). Similar smaller scale NMR tube experiments using ethanol and methanol as substrates yielded proportional amounts of acetaldehyde and formalydehyde respectively (Table S2).

The kinetics of the AAD reaction of methanol to formaldehyde were studied using time-resolved NMR spectroscopy. An NMR tube containing catalyst **1Br**, photosensitizer, DMEA, and methanol in CD_3CN was irradiated, and spectra were acquired over several hours. This allowed for real-time monitoring of the reaction without disturbing the system. The reduction in the concentration of methanol was quantified, enabling the construction of a time

Table 2 Summary of the photocatalytic dehydrogenation of alcohols with [Ni(2,6-$(Ph_2PNH)_2(NC_5H_3)$)Br]Br, **1Br**. Irradiation of 4 mL DMA solutions of **1Br** and 2 mM $Ru(bpy)_3(PF_6)_2$ with DMEA as the electron donor (ED) and 1 mL of added ROH. Irradiated with a visible blue light LED under N_2 for 24 h

Entry	[**1Br**] (mM)	ROH	H_2 (μmol)	TON
1	2	^{i}PrOH	342	34
2	2	EtOH	369	37
3	2	NpOH	272	27
4	2	CD_3OH	456[a]	46

[a] Observed HD and D_2 by mass spectrometry.

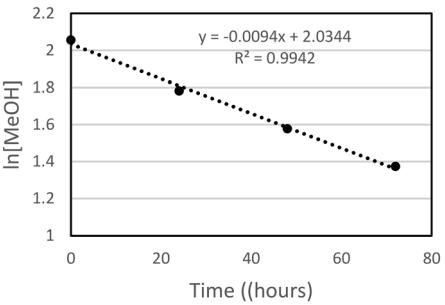

Fig. 1 Time-dependent photocatalytic conversion of methanol to formaldehyde and H_2 (AAD) catalyzed by **1Br** with $Ru(bpy)_3(PF_6)_2$ and DMEA conducted in CD_3CN. Data points represent concentrations of ln[MeOH] over time, demonstrating first-order kinetics. The equation represents a linear fit to the data.

Open Access Article. Published on 11 2568. Downloaded on 17/5/2569 10:50:58.
This article is licensed under a Creative Commons Attribution-NonCommercial 3.0 Unported Licence.

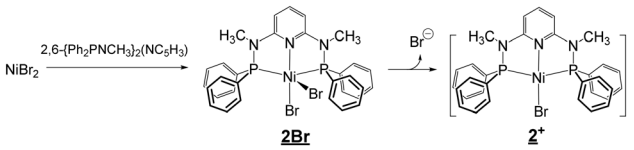

Scheme 3 Preparation and structural representation of complex $\mathbf{2}^{+}$.

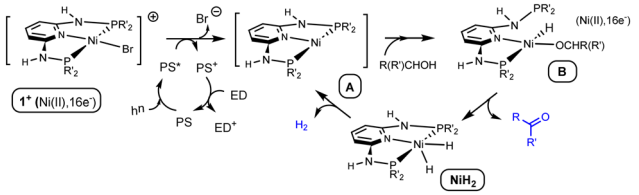

Scheme 4 Proposed mechanism for the photocatalytic molecular acceptorless dehydrogenation of alcohols with [Ni(2,6-$(Ph_2PNH)_2(NC_5H_3)$)Br]$^{+}$. PS = $Ru(bpy)_3^{2+}$, ED = DMEA.

profile for the transformation (Fig. 1). The data analysis revealed a first-order rate dependence on [MeOH] with a rate constant of $9.4(10^{-3})$ h^{-1}.

In an effort to to reveal the general features of this process and to explore potential mechanisms we prepared our previously reported the analogous complex **2Br**. When dissolved, this complex dissociates a bromo ligand to yield $\mathbf{2}^{+}$ (Scheme 3).[41]

We were pleased to observe successful photocatalytic AAD with the same set of alcohols and similar performance using the optimized conditions observed with $\mathbf{1}^{+}$ with this data presented in Table 2. These results broaden the reaction scope and suggest the lack of direct involvement of ligand NH groups in the catalytic process (Table 3).

Based on our experimental data and previous work with these complexes, we propose a mechanism for photocatalyzed AAD shown in Scheme 4. Our previous studies demonstrated that $\mathbf{1}^{+}$ undergoes a reversible reduction at $E_{1/2}$ = −0.93 V and two irreversible reductions at −1.4 V and −2.49 V (all potentials referenced to the ferrocene/ferrocenium couple).[41] When converted to SCE reference, these potentials correspond to approximately −0.62 V, −1.1 V, and −2.18 V *vs.* SCE, respectively. Considering that the Ru(II)/(I) couple for $Ru(bpy)_3^{2+}$ has a reported reduction potential of −1.33 V *vs.* SCE, only the first two reductions of $\mathbf{1}^{+}$ are accessible in this photoredox system.

We propose a catalytic cycle initiating with the double reduction of $\mathbf{1}^{+}$, followed by bromide anion loss, yielding compound **A**. The reducing equivalents are supplied by $Ru(bpy)_3^{+}$, which is generated through photoexcitation of $Ru(bpy)_3^{2+}$ and subsequent reductive quenching by DMEA. This 16-electron Ni(0) complex is primed for oxidative addition of the alcohol O–H bond.

Computational optimization of the oxidative addition product of **A** with methanol revealed dissociation of one aminophosphine group, with a new hydride ligand occupying the vacated coordination site, resulting in complex **B** (Fig. 2). The transformation of the PN^3P ligand to a bidentate PN configuration exploits a crucial feature of the pincer framework: it creates the necessary open coordination environment at the Ni center, a key prerequisite for β-hydrogen elimination.[47] This structural change facilitates β-hydrogen elimination from **B**, resulting in a Ni(II) dihydride ($\mathbf{NiH_2}$) intermediate. Our previous work demonstrated that analogous pincer-stabilized dihydrides readily convert to dihydrogen complexes, followed by H_2 elimination.[48]

Importantly, an alternative outer-sphere mechanism could also be proposed. In general, such mechanisms involve either an anionic ligand or hydrogen bonding between the substrate and a ligand that orient the substrate and metal center for reaction.[14–16] In the case of complex $\mathbf{1}^{+}$ the neutral nature of the ligand and the spatial orientation of the N–H moieties, planar and directed away from the metal center, do not favor an outer-sphere mechanism. An alternative outer-sphere mechanism involving deprotonation of an N–H function in species **A** to produce species **X** (along with its resonance structures) was also considered. Both **A** and **X** were computationally optimized using DFT with a B3LYP functional and def2TZVP basis set employing a polarized continuum model with parameters for acetonitrile. The resultant optimizations indicated that proposed compound **X** was higher in energy than **A** by more than 200 kcal and further discourage an alternative outer-sphere mechanism. Finally, the observation of similar catalytic reactivity for photocatalytic AAD using $\mathbf{2}^{+}$ also disfavor this option.

Table 3 Summary of the photocatalytic dehydrogenation of alcohols with [Ni(2,6-$(Ph_2PNMe)_2(NC_5H_3)$)Br]$^{+}$, $\mathbf{2}^{+}$. Irradiation of 4 mL DMA solutions of $\mathbf{2}^{+}$ and 2 mM $Ru(bpy)_3(PF_6)_2$ with DMEA as the electron donor (ED) and 1 mL of added ROH. Irradiated with a visible blue light LED under N_2 for 24 h

Entry	[$\mathbf{2}^{+}$] (mM)	ROH	H_2 (μmol)	TON
1	2	CH_3OH	433	43
2	2	^{i}PrOH	356	35
3	2	EtOH	368	37
4	2	NpOH	265	27

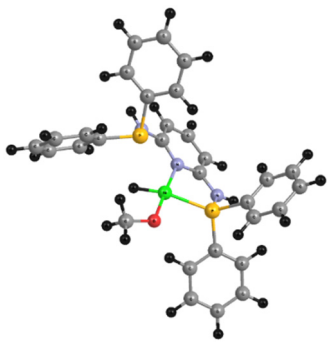

Fig. 2 Computationally optimized oxidative addition product of **A** and the methanol. Obtained using the B3LYP functional, def2TZVP basis set and PCM model for solvation in acetonitrile.

This journal is © The Royal Society of Chemistry 2025

Open Access Article. Published on 11 2568. Downloaded on 17/5/2569 10:50:58.
This article is licensed under a Creative Commons Attribution-NonCommercial 3.0 Unported Licence.

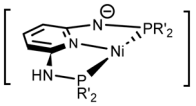

X

The computed ΔG for this proposed reaction cycle using species A was found to be 26.1 kcal mol^{-1} (Table S3). This can be directly compared with the free energy calculation using the ΔG_f values of for gaseous methanol (−38.8 kcal mol^{-1}) and gaseous formaldehyde (−24.5 kcal mol^{-1}) yielding a ΔG of 14.3 kcal mol^{-1}.[49] The discrepancy in the required energy for this conversion corresponds well with the energy available by the Ru(II)/(I) redox couple for the photosensitizer $Ru(bpy)_3^{2+}$ (E_{red} = −1.33 V *vs.* SCE) which is equivalent to about 25.1 kcal mol^{-1}. Attempts to observe intermediates in this mechanism by examining a reacting system by ^{31}P NMR gave $\mathbf{1}^+$ as the only significant and clear NMR signal suggesting that this is the resting state of the catalyst system.

Conclusions

In this report, we have demonstrated the first examples of a well-characterized, air-stable nickel complexes $[Ni(2,6\text{-}\{Ph_2PNR\}_2(NC_5H_3))Br]^+$ (R = H, $\mathbf{1}^+$; R = Me, $\mathbf{2}^+$) that function as exceptional homogeneous visible-light photoredox catalysts for acceptorless alcohol dehydrogenation (AAD). This system operates under mild conditions, including room temperature and visible light irradiation, to selectively produce hydrogen from various aliphatic alcohols. The introduction of dimethylethanolamine (DMEA) as a novel, efficient electron donor further enhances the system's performance and practicality.

Our work addresses key challenges in sustainable hydrogen production, offering a promising approach that aligns with the urgent need for clean energy solutions. The use of a 3d metal catalyst represents a significant step towards more economical and environmentally friendly hydrogen generation. Furthermore, the mechanistic insights gained from this study, including the crucial role of the flexible pincer ligand, open new avenues for designing improved catalysts for photoredox AAD.

This research not only advances our understanding of photocatalytic hydrogen production but also bridges the gap between traditional catalysis and photoredox chemistry. As we continue to face global energy challenges, such innovative approaches to hydrogen generation from renewable resources will play a vital role in shaping a sustainable energy future.

Author contributions

E. M.: conceptualization, data curation, investigation, writing – review and editing. D. R.: conceptualization, analysis, funding acquisition, writing – original draft.

Conflicts of interest

There are no conflicts to declare.

Data availability

The data supporting this article have been included as part of the SI. See DOI: https://doi.org/10.1039/D5CY00647C.

Acknowledgements

We acknowledge funding from NSERC of Canada. EM acknowledges funding from the Libyan-North American Scholarship Program (LNASP).

Notes and references

1 *Global Hydrogen Review*, International Energy Agency, Paris, 2022.
2 C. Acar, I. Dincer and G. F. Naterer, *Int. J. Energy Res.*, 2016, **40**, 1449–1473.
3 I. Dincer and C. Acar, *Int. J. Energy Res.*, 2015, **39**, 585–606.
4 A. Haryanto, S. Fernando, N. Murali and S. Adhikari, *Energy Fuels*, 2005, **19**, 2098–2106.
5 L. Tong, R. Zong and R. P. Thummel, *J. Am. Chem. Soc.*, 2014, **136**, 4881.
6 K. Sordakis, C. Tang, L. K. Vogt, H. Junge, P. J. Dyson, M. Beller and G. Laurenczy, *Chem. Rev.*, 2018, **118**, 372–433.
7 M. Nielsen, H. Junge, A. Kammer and M. Beller, *Angew. Chem., Int. Ed.*, 2012, **51**, 5711–5713.
8 S. S. Lokras, P. K. Deshpande and N. R. Kuloor, *Ind. Eng. Chem. Proc. Design Dev.*, 1970, **9**, 293–297.
9 R. H. Crabtree, *Chem. Rev.*, 2017, **117**, 9228–9246.
10 M. Trincado, J. Bösken and H. Grützmacher, *Coord. Chem. Rev.*, 2021, **443**, 213967.
11 D. Borah, A. Sharma, R. R. Dutta, I. Bhuyan and R. Dutta, *J. Organomet. Chem.*, 2025, **1024**, 123445.
12 S. Kostera and L. Gonsalvi, *ChemSusChem*, 2025, **18**, e202400639.
13 P. K. Verma, *Coord. Chem. Rev.*, 2022, **472**, 214805.
14 G. A. Filonenko, R. Van Putten, E. J. M. Hensen and E. A. Pidko, *Chem. Soc. Rev.*, 2018, **47**, 1459–1483.
15 L. Alig, M. Fritz and S. Schneider, *Chem. Rev.*, 2019, **119**, 2681–2751.
16 K. Das, S. Waiba, A. Jana and B. Maji, *Chem. Soc. Rev.*, 2022, **51**, 4386–4464.
17 W. Qi, N. Wang, L. Qin, P. Yu and Z. Zheng, *ACS Catal.*, 2024, **14**, 3434–3445.
18 M. Nielsen, E. Alberico, W. Baumann, H. J. Drexler, H. Junge, S. Gladiali and M. Beller, *Nature*, 2013, **495**, 85–89.
19 A. Agapova, H. Junge and M. Beller, *Chem. – Eur. J.*, 2019, **25**, 9345–9349.
20 P. Hu, Y. Diskin-Posner, Y. Ben-David and D. Milstein, *ACS Catal.*, 2014, **4**, 2649–2652.
21 J. Luo, S. Kar, M. Rauch, M. Montag, Y. Ben-David and D. Milstein, *J. Am. Chem. Soc.*, 2021, **143**, 17284–17291.

Open Access Article. Published on 11 2568. Downloaded on 17/5/2569 10:50:58.
This article is licensed under a Creative Commons Attribution-NonCommercial 3.0 Unported Licence.

22 V. Arora, E. Yasmin, N. Tanwar, V. R. Hathwar, T. Wagh, S. Dhole and A. Kumar, *ACS Catal.*, 2023, **13**, 3605–3617.
23 D. Benito-Garagorri and K. Kirchner, *Acc. Chem. Res.*, 2008, **41**, 201–213.
24 A. Bruneau-Voisine, D. Wang, T. Roisnel, C. Darcel and J. Sortais, *Catal. Commun.*, 2017, **92**, 1–4.
25 S. Chakraborty, P. E. Piszel, W. W. Brennessel and W. D. Jones, *Organometallics*, 2015, **34**, 5203–5206.
26 M. C. Morrow and C. W. Machan, *Chem. Commun.*, 2025, **61**, 7710–7723.
27 T. Gunasekara, Y. Tong, A. L. Speelman, J. D. Erickson, A. M. Appel, M. B. Hall and E. S. Wiedner, *ACS Catal.*, 2022, **12**, 2729–2740.
28 Y. C. Liu, D. X. Cao, Q. Y. Ban, W. J. Ma and B. Xiao, *Chem. Commun.*, 2025, **61**, 6917–6920.
29 H. Fuse, H. Mitsunuma and M. Kanai, *J. Am. Chem. Soc.*, 2020, **142**, 4493–4499.
30 H. N. Kagalwala, A. B. Maurer, I. N. Mills and S. Bernhard, *ChemCatChem*, 2014, **6**, 3018–3026.
31 J. J. Zhong, W. P. To, Y. Liu, W. Lu and C. M. Che, *Chem. Sci.*, 2019, **10**, 4883–4889.
32 Z. Chai, *Chem. – Asian J.*, 2021, **16**, 460–473.
33 L. Ibáñez-Ibáñez, G. Guisado-Barrios and J. A. Mata, *J. Catal.*, 2025, **448**, 116134.
34 X. J. Yang, L. Q. Zheng, L. Z. Wu, C. H. Tung and B. Chen, *Green Chem.*, 2019, **21**, 1401–1405.
35 H. Li, B. Zheng and K.-W. Huang, *Coord. Chem. Rev.*, 2015, **293–294**, 116–138.
36 H. Li, T. P. Goncalves, Q. Zhao, D. Gong, Z. Lai, Z. Wang, J. Zheng and K. Huang, *Chem. Commun.*, 2018, **54**, 11395.
37 H. Li, J. Hu, Q. Zhao, D. Gong, Z. Lai, Z. Wang, J. Zheng and K. Huang, *J. Org. Chem.*, 2018, **83**, 14969–14977.
38 D. Lupp and K. W. Huang, *Organometallics*, 2020, **39**, 18–24.
39 G. K. Rao, W. Pell, B. Gabidullin, I. Korobkov and D. Richeson, *Chem. – Eur. J.*, 2017, **23**, 16763–16767.
40 J. Brown, J. Ovens and D. Richeson, *ChemSusChem*, 2022, **15**, e202102542.
41 S. Norouziyanlakvan, G. K. Rao, J. Ovens, B. Gabidullin and D. Richeson, *Chem. – Eur. J.*, 2021, **27**, 13518–13522.
42 Y. Pellegrin and F. Odobel, *C. R. Chim.*, 2017, **20**, 283–295.
43 W. Xue, J. Ye, Z. Zhu, R. Kumar and J. Zhao, *Energy Environ. Sci.*, 2025, **18**, 214–226.
44 F. M. De Souza, P. K. Kahol and R. K. Gupta, *ACS Symp. Ser.*, 2021, **1380**, 1–24.
45 A. Gautam and M. Kumar Mondal, *Fuel*, 2023, **331**, 125864.
46 J. Wang, P. Yang, B. Cao, J. Zhao and Z. Zhu, *Appl. Surf. Sci.*, 2015, **325**, 86–90.
47 S. Z. Tasker, E. A. Standley and T. F. Jamison, *Nature*, 2014, **509**, 299–309.
48 S. Norouziyanlakvan, J. Ferguson and D. Richeson, *Catal. Sci. Technol.*, 2022, **12**, 7494–7500.
49 *Lange's Handbook of Chemistry*, ed. J. A. Dean, McGraw-HIll Inc., New York, 15th edn, 1999.

 This journal is © The Royal Society of Chemistry 2025